Molecular Crystal Structures and Nonlinear Optical Properties in the Series of Dicyanovinylbenzene and Its Derivatives

Mikhail Yu. Antipin,*[†,‡] Tatiana V. Timofeeva,[†,‡] Ronald D. Clark,[†] Vladimir N. Nesterov,[‡] Mohan Sanghadasa,[§] Thomas A. Barr,[§] Benjamin Penn,[||] Leonard Romero,[†] and Melvin Romero[†]

Department of Physical Sciences, New Mexico Highlands University, Las Vegas, New Mexico 87701, Institute of Organoelement Compounds, Russian Academy of Sciences, 28 Vavilov St., B-334 Moscow, Russia, University of Alabama in Huntsville, Huntsville, Alabama 35899, and NASA George C. Marshall Space Flight Center, Huntsville, Alabama 35812

Received: January 6, 1998; In Final Form: July 1, 1998

X-ray single-crystal structures, molecular mechanics (MM) calculations of the optimal molecular dimers, and calculations of the static second-order polarizabilities (β) were performed for a large series of methoxy- and dimethylamino-substituted derivatives of dicyanovinylbenzene and some of its analogues having large values of the molecular nonlinear optical susceptibilities. X-ray structural analysis has been performed for 3,4-dimethoxy- and 3,4,5-trimethoxy-dicyanovinylbenzenes (**I, II**), *p*-(dimethylamino)-dicyanovinylbenzene (**III**), 1,1-dicyano-2-phenyl-2-(2-methoxyphenyl)ethene ($2\text{-MeO}-C_6H_4-C(C_6H_5)=C(CN)_2$) (**IV**), and 4-(4-methoxyphenyl)-1,1-dicyano-1,3-butadiene ($4\text{-MeO}-C_6H_4-CH=CH-CH=C(CN)_2$) (**V**). Crystal packing analysis and energetic MM calculations revealed the factors responsible for the formation of the centrosymmetric crystals. Compounds **III** and **V** were found to form acentric crystal structures (space groups $P2_1$ and Pc, respectively) and therefore are capable to the second-harmonic generation (SHG) in solid state. Qualitative data have demonstrated that compound **V** is rather active in SHG in the powder state (using Nd:YAG laser with $\lambda = 1064$ nm) that may be important for its application. On the contrary, the powder of **III** is not active in SHG despite the “optimal” crystal packing that might be related to the strong absorption of the second harmonic light at $\lambda = 532$ nm, but this compound gives strong SHG signal using the laser light with $\lambda = 1907$ nm. Analysis of the influence of the different substituents in the aromatic ring on the calculated β values in the series of the compounds studied was made.

Introduction

Nonlinear optical (NLO) properties of organic molecules are the subject of very intensive studies in recent years because of their potential applicability for electrooptical modulation, frequency mixing, SHG (second-harmonic generation), and fabrication of many optical devices.[1,2] Owing to their much larger molecular nonlinearities, very fast optical response times, and higher optical damage thresholds as compared with the well-known inorganic materials,[3] organic compounds offer several advantages for these devices. Substituted aromatic compounds with both π-electron-donating and π-electron-accepting groups, such as the “classical” NLO chromophore 2-methyl-4-nitroaniline,[4] are the most typical organic nonlinear optical materials which have been studied. Many other classes of numerous aromatic and unsaturated organic, heterocyclic, organoelement, and organometallic compounds have also been studied as prospective materials for possible NLO applications.[5,6] Some of these materials were found to have very large molecular second-order optical susceptibilities (see, for instance, refs 7 and 8), exceeding many times those for more simple aromatics.

On the other hand, there are a few severe restrictions for practical NLO application of material under consideration. For instance, second-harmonic generation in the solid state is possible only if a given compound forms an acentric crystal structure (i.e., its crystals belong to a noncentrosymmetric space group). This necessary requirement is not sufficient, however. The efficiency of a nonlinear optical response depends strongly on the molecular orientation (namely, orientation of its dipole moment or charge-transfer axis) with respect to the polar crystal axes, and for a given crystal symmetry there are some “optimal” orientation angles[9] maximizing NLO responses. There are some examples in the literature (for instance, in the case of *p*-nitrodimethyaniline[10] having acentric space group $P2_1$), when molecules with rather high second-order nonlinearities form crystal structures with nonoptimal molecular orientations even in the acentric space groups. Some other important requirements to materials for displaying useful and effective NLO properties are the short wavelength cutoff in optical spectra,[11] thermal stability, availability of a given compound, etc. All these requirements restrict strongly the number of possible compounds for NLO applications, and therefore systematical studies of the large series of the parent chromophore compounds have great importance in the modern NLO material design.

Such a design includes usually a few steps, namely, theoretical estimation of the molecular nonlinear optical susceptibility (values of β and/or γ, the second- and third-order polarizability tensors) using different quantum-chemical approaches, chemical synthesis of the compounds under interest and their single-crystal growth, study of the optical and NLO properties in solution and in solid state, and X-ray structural analysis. Of course, any prior estimation of NLO properties of some compound (or

---

[†] New Mexico Highlands University.

[‡] Russian Academy of Sciences.

[§] University of Alabama.

[||] NASA George C. Marshall Space Flight Center.

S1089-5639(98)00676-8 CCC: $15.00

a series of compounds) has great importance in the molecular engineering of new NLO materials. But, while calculation (estimation) of the β and γ values is a rather well-developed and optional procedure in many quantum-chemical program packages, a prediction of the crystal structure of a given compound (centric or acentric) is still a very difficult problem, being far from the general solution (for some discussions on this subject, see refs 12−15). Therefore an important and necessary step in NLO material design is an X-ray structural analysis of organic chromophores together with development of different theoretical approaches for their crystal structure prediction.

Single-crystal X-ray diffraction analysis has great significance in NLO material studies because it allows one to determine very simply and unequivocally a crystal space group and symmetry, as well as molecular conformation and molecular geometry features that might be responsible for molecular and crystalline NLO characteristics. In addition, modern opportunities of the high-resolution single-crystal X-ray diffraction method may provide information about electronic properties of molecules in crystals (charge distributions and related quantities, such as dipole and higher multipole moments, etc.[16]) that are responsible for exhibiting high NLO characteristics.

In our previous paper[17] we reported X-ray crystal structures, molecular mechanics calculations, and calculations of the nonlinear polarizabilities (β and γ) for dicyanovinylbenzene and a series of some of its methoxy-substituted derivatives (with *o*-methoxy, *p*-methoxy, and 2,4-dimethoxy substituents). This class of organic chromophores represents an interest in NLO material studies because of the well-known efficiency of the $-CH=C(CN)_2$ group as an electron acceptor with an extended conjugation chain.[18] In addition, the presence of this group increases the thermal stability of organic compounds.

It was shown[17] that among the four compounds studied only *o*-methoxy-dicyanovinylbenzene, also known as DIVA, has an acentric crystal space group ($P2_1$) and therefore exhibits NLO properties in the solid state.[19,20] The corresponding para-substituted derivative and 2,4-dimethoxy analogue (having much higher molecular second-order optical responses β) were found to form centrosymmetric crystal structures. Crystal packing analysis of the structures studied together with the molecular mechanics energetic calculations of the possible molecular dimers showed that the stacking interactions in centrosymmetric dimers as well as in-plane interactions such as weak C−H···N hydrogen bonds (C−H bond belongs to the dicyanovinyl group $-CH=C(CN)_2$) probably prevent the crystal acentricity. Introduction of the *o*-methoxy substituent into the molecule of dicyanovinylbenzene does not increase the value of β in accord with calculations and experimental measurements in solution, but it inhibits formation of the above-mentioned H-bonded dimers giving the crystal structure of DIVA. For 2,4-dimethoxy-dicyanovinylbenzene, the formation of antiparallel centrosymmetric dimers of the stacking-type was found to be preferable, and this compound also forms centrosymmetric crystals.

Theoretical calculations of the β values performed in ref 17 for some other dimethoxy-substituted dicyanovinylbenzenes showed also that for 2,4- and 3,4-isomers the β values are very similar and close to that for the *p*-methoxy-substituted analogue. So, the main contribution in β is introduced by the MeO substituent in the para-position of the aromatic ring. Therefore preparation, crystal structure analysis, and study of NLO properties of some other derivatives of this series with the donor substituents (methoxy or dimethylamino) in the para-position to the dicyanovinyl group may have interest in the search of new NLO-active materials.

Taking this into account in the present paper, we report molecular and crystal structures and calculated values of the second-order polarizabilities (β) for the series of new compounds, including 3,4-dimethoxy-dicyanovinylbenzene (3,4-$(MeO)_2-C_6H_3-CH=C(CN)_2$) (**I**), 3,4,5-trimethoxy-dicyanovinylbenzene (3,4,5-$(MeO)_3-C_6H_2-CH=C(CN)_2$) (**II**), and *p*-(dimethylamino)-dicyanovinylbenzene ($4\text{-}Me_2N-C_6H_4-CH=C(CN)_2$) (**III**). To estimate the influence of phenyl substituent at the carbon atom of the dicyanovinyl group on the molecular conformation and geometry of the dicyanovinylbenzene moiety, we also studied the molecular and crystal structures of 1,1-dicyano-2-phenyl-2-(2-methoxyphenyl)ethene ($2\text{-}MeO-C_6H_4-C(C_6H_5)=C(CN)_2$) (**IV**). Finally, hyperpolarizability calculations were performed for a series of related compounds having longer conjugated chains, which are considered to be more effective NLO materials.[18] Crystal data for one (noncentrosymmetric) representative of this series, namely, 4-(4-methoxyphenyl)-1,1-dicyano-1,3-butadiene ($4\text{-}MeO-C_6H_4-CH=CH-C=C(CN)_2$) (**V**), are presented. For compounds **III** and **V** forming acentric crystal structures, experimental values of the second-order susceptibilities were measured in solution, and the powder SHG test for these two compounds was applied as well.

We should note that a very short communication about NLO properties in solid state and X-ray analysis of compound **III** was published earlier;[21] however, no important structural details including crystal data and atomic coordinates were published in this paper.

An additional purpose of the present publication is an estimation of the plausibility of the theoretical approach (described in detail in ref 17) for prediction of the possible centric/acentric packing arrays in crystals of the compounds of interest. This simple approach is based on calculations of the relative energies of the possible molecular dimers using molecular mechanics technique. In our opinion, in some cases these rather simple calculations may give an answer about possible formation of the acentric crystal, and the series of the compounds studied is a good test to check the workability of this approach.

Experimental Section and Calculational Details

Synthesis of the dicyanovinylbenzene derivatives **I**−**III** and the dicyanobutadiene derivative **V** were performed by adaptation of the method reported in ref 22. In this procedure, appropriate benzaldehydes or cinnamaldehydes were condensed with malononitrile in absolute ethanol to yield the desirable derivatives. The synthetic route used for the preparation of the dicyanophenylethene derivative **IV** was adapted from ref 23, in which phenyllithium was allowed to react with 2-methoxybenzonitrile in the presence of malononitrile.

X-ray Analysis. Single crystals of **I**−**V** suitable for X-ray analysis were grown by slow crystallization from different solvents. Most difficult was the single-crystal growth for compounds **III** and **V** because of formation of irregular twins, and numerous attempts were made in order to obtain suitable samples for X-ray analysis. Crystal twinning prevented obtaining of the accurate diffraction data for these compounds, but their molecular and crystal structures (crystal packing arrays) were proven without any doubt.

All experimental data were obtained with the 4-circle automatic X-ray diffractometers Syntex $P2_1$ (compounds **I**−**III**) and Siemens P3/PC (compounds **IV, V**) using Mo Kα radiation ($\lambda = 0.7107$ Å) and graphite monochromator at 193 K (**I**−**III**)

TABLE 1: Structure Determination Summary for Compounds I−V

	I	II	III	IV	V
empirical formula	$C_{12}H_{10}N_2O_2$	$C_{13}H_{12}N_2O_3$	$C_{12}H_{11}N_3$	$C_{17}H_{12}N_2O$	$C_{13}H_{10}N_2O$
formula weight	214.2	244.3	197.2	260.3	210.2
crystal size (mm)	0.2 × 0.4 × 0.4	0.2 × 0.2 × 0.2	0.1 × 0.1 × 0.4	0.3 × 0.3 × 0.4	0.1 × 0.1 × 0.5
crystal system	triclinic	monoclinic	monoclinic	monoclinic	monoclinic
space group	*P*-1	$P2_1/c$	$P2_1$	$P2_1/n$	Pc
unit cell dimensions:					
a (Å)	7.501(2)	3.914(2)	3.951(4)	8.394(2)	3.957(2)
b (Å)	8.892(3)	14.192(7)	14.078(11)	8.357(2)	13.832(4)
c (Å)	9.223(2)	22.374(9)	9.499(9)	20.036(4)	10.392(5)
α (deg)	93.77(2)	90.0		90.0	
β (deg)	105.44(2)	91.35(4)	99.88(8)	93.97(2)	94.11(3)
γ (deg)	110.23(2)	90.0		90.0	
volume ($Å^3$)	547.9(3)	1242.5(9)	520.5(8)	1402.1(6)	567.4(4)
Z	2	4	2	4	2
density (calc, g/cm^3)	1.299	1.306	1.259	1.233	1.231
absorption coefficient (mm^{-1})	0.091	0.095	0.078	0.078	0.080
F(000)	224	512	208	544	220
diffractometer used	Syntex $P2_1$	Syntex $P2_1$	Syntex $P2_1$	Siemens	Siemens
temperature (K)	193(2)	193(2)	193(2)	297(2)	297(2)
2θ range (deg)	2.0−56.0	2.0−45.0	2.0−44.0	2.0−56.0	2.0−44.0
scan range (ω, deg)	1.90	1.80		2.00	
number of reflections					
collected	2854	1872	810	4197	1176
independent	2653	1592	810	3182	1176
observed ($F > 4\sigma$)	1786	1536	656	2266	689
no. of parameters refined	185	211	136	229	143
data-to-param ratio	9.7	7.3	4.8	9.9	3.9
final *R* indices	0.0467	0.0697	0.0984	0.0544	0.1295
final *wR* indices	0.0604	0.1530	0.1437	0.0780	0.1419
goodness of fit	2.00	1.05	2.54	1.25	1.30

and room temperature (**IV, V**). The structures were solved by direct methods and refined by full-matrix least-squares in the anisotropic (non-hydrogen atoms) approximation. Hydrogen atom positions were calculated geometrically or were found with difference Fourier synthesis. All these atoms were refined in the isotropic approximation (except for structures **III** and **V** where a riding model was used). Absorption correction was not applied because it was small, and extinction correction was found to be negligible. All calculations were performed with a personal computer using SHELXTL PLUS program package. Important details of the crystal data, data collection, and structure solution and refinement are summarized in Table 1. Non-hydrogen atom coordinates and their isotropic equivalent displacement parameters are given in Table 2, and bond lengths and bond angles are presented in Table 3. General view of the structures studied with the atomic numbering schemes is shown in Figures 1 and 2. Full structural details of the X-ray analysis are deposited in the Supporting Information.

Energetic Calculations of the Molecular Dimers. The energy of the molecular dimers was calculated for compounds **I**−**III** and **V** with the MM3 program package using stochastic search procedure.[24] The total energy was calculated as a sum of the intra- and intermolecular interactions. Stochastic procedure has some advantages in comparison with mapping of the intermolecular energy as a function of interplanar distance and in-plane rotation angle as described by Itoh et al.[25a,b] because the molecular conformations and relative molecular orientations in dimers were not restricted during optimization. Three types of dimers were taken into account with the parallel, centrosymmetric C_i, and C_2 symmetries as starting points for a stochastic search. In most cases the dimers preserved starting molecular orientation during optimization. The top list of the dimer energies calculated for compounds **I**−**III** and **V** is presented in Table 4.

Calculation of the Static Polarizabilities (*β*). To calculate important NLO molecular electronic characteristics (dipole moments and second-order polarizabilities β) we have used the technique described in detail in our previous paper.[17] It was shown that the values of β calculated with the experimental X-ray geometries, as well as obtained using quantum-chemical or molecular mechanics optimized geometry parameters, are very close in most cases. So, the easiest way to estimate a priori some molecular electronic properties for a large series of compounds is the molecular mechanics calculation of the optimal molecular geometry and semiempirical quantum-chemical calculation of their electronic properties. The same approach (molecular mechanics for the geometry calculations and semiempirical quantum-chemical approximation for hyperpolarizability estimations) was published recently.[26]

Calculations of the conformation and geometry parameters of all molecules under investigation in the free state were performed using the MM3 program package.[27,28] For the computation of the second-order polarizabilities a modification of the static field method[29] (developed in refs 30 and 31) was used. In each case, 252 static field calculations were obtained (MOPAC program, AM1) which were analyzed by the HYPER program.[32a] Results of these calculations for two groups of compounds (**I**−**XV**) with the dicyanovinyl ($-CH{=}C(CN)_2$) and 1,1-dicyano-1,3-butadiene ($-CH{=}CH-CH{=}C(CN)_2$) long-chain fragments and different ($-OMe$, $-NMe_2$, and $-NEt_2$) substituents in the aromatic rings are presented in Tables 5 and 6. For two molecules (**III** and **V**) an ab initio (STO-3G basis sets) quantum-chemical calculation of the molecular geometry and dipole moments was performed using the GAUSSIAN program. In our calculations we did not take into account the influence of the solvent on the hyperpolarizability values although it is known (see, for example, ref 32b) that for "classic" aromatic chromophores in polar solvents (in particular, DMSO, ($\epsilon = 45$), including as well compound **III**, it may increase the values of β by a factor as great as 3−6 upon changing from vacuum to solvent environment. We may suggest, however, that for such a nonpolar solvent as 1,4-dioxane ($\epsilon = 2.21$) that

TABLE 2: Atomic Coordinates (×10^4) for Non-Hydrogen Atoms and Equivalent Isotropic Displacement Parameters (Å^2, × 10^3) in I−V^a

	x	*y*	*z*	*U*(eq)		*x*	*y*	*z*	*U*(eq)
					Structure **I**				
O(1)	3621(2)	7713(1)	1435(1)	41(1)	C(5)	646(3)	3757(2)	2034(2)	38(1)
O(2)	3375(2)	4762(1)	952(1)	42(1)	C(6)	−626(3)	4127(2)	2704(2)	40(1)
N(1)	−4791(2)	7360(2)	5399(2)	48(1)	C(7)	−1922(3)	6001(2)	3672(2)	37(1)
N(2)	−1003(3)	9999(2)	2862(2)	52(1)	C(8)	−2360(2)	7334(2)	3881(2)	35(1)
C(1)	−564(2)	5718(2)	2948(2)	35(1)	C(9)	−3722(3)	7346(2)	4724(2)	39(1)
C(2)	876(2)	6952(2)	2504(2)	35(1)	C(10)	−1586(3)	8817(2)	3315(2)	38(1)
C(3)	2142(2)	6596(2)	1854(2)	34(1)	C(11)	3784(4)	9365(2)	1679(3)	55(1)
C(4)	2049(3)	4976(2)	1598(2)	35(1)	C(12)	3377(4)	3148(2)	711(2)	45(1)
					Structure **II**				
O(1)	−3947(9)	6730(2)	2448(1)	42(1)	C(5)	−493(11)	8580(3)	1526(2)	28(1)
O(2)	−2768(9)	8608(2)	2503(1)	43(1)	C(6)	386(12)	8115(3)	1016(2)	30(1)
O(3)	−200(8)	9541(2)	1601(1)	40(1)	C(7)	994(12)	6565(3)	483(2)	31(1)
N(1)	4895(13)	8433(3)	−331(2)	58(1)	C(8)	2700(13)	6785(3)	−22(2)	34(1)
N(2)	4269(12)	5473(3)	−765(2)	54(1)	C(9)	3847(14)	7708(4)	−192(2)	41(1)
C(1)	−38(12)	7137(3)	980(2)	31(1)	C(10)	3501(13)	6054(3)	−438(2)	38(1)
C(2)	−1517(13)	6661(3)	1460(2)	33(1)	C(11)	−4709(19)	5727(3)	2409(3)	42(1)
C(3)	−2476(12)	7123(3)	1968(2)	32(1)	C(12)	−964(21)	8376(5)	3050(2)	55(2)
C(4)	−1857(12)	8111(3)	2008(2)	31(1)	C(13)	1244(19)	10073(4)	1121(3)	47(2)
					Structure **III**				
N(1)	−2643(25)	−1380(9)	1229(11)	49(4)	C(6)	36(23)	857(10)	2834(10)	35(3)
N(2)	−8515(21)	0	−2508(11)	47(3)	C(7)	−3444(20)	1082(10)	399(11)	30(3)
N(3)	5043(23)	2592(9)	5262(10)	36(3)	C(8)	−4513(22)	200(10)	−48(12)	36(3)
C(1)	−1276(22)	1423(9)	1646(11)	30(3)	C(9)	−3491(25)	−665(10)	716(14)	40(4)
C(2)	−402(22)	2395(10)	1748(10)	31(3)	C(10)	−6727(22)	76(9)	−1413(11)	33(3)
C(3)	1656(24)	2800(10)	2878(11)	35(3)	C(11)	5825(27)	3611(11)	5360(14)	45(4)
C(4)	2997(19)	2212(10)	4067(11)	28(3)	C(12)	6429(22)	2025(10)	6486(10)	33(3)
C(5)	2170(19)	1237(10)	4029(10)	32(3)					
					Structure **IV**				
O(1)	2939(2)	4217(2)	1137(1)	61(1)	C(8)	−869(2)	2112(2)	962(1)	50(1)
N(1)	−1356(3)	1892(4)	2210(1)	99(1)	C(9)	−1114(2)	1971(3)	1662(1)	65(1)
N(2)	−3512(2)	2394(3)	250(1)	90(1)	C(10)	−2317(2)	2291(3)	549(1)	61(1)
C(1)	1956(2)	1635(2)	1244(1)	43(1)	C(11)	4182(4)	5361(4)	1243(2)	90(1)
C(2)	3163(2)	2746(2)	1411(1)	46(1)	C(12)	1010(2)	2316(2)	45(1)	44(1)
C(3)	4449(2)	2303(3)	1847(1)	56(1)	C(13)	63(2)	3242(2)	−403(1)	50(1)
C(4)	4532(3)	784(3)	2108(1)	62(1)	C(14)	483(3)	3453(3)	−1055(1)	59(1)
C(5)	3329(3)	−311(3)	1959(1)	66(1)	C(15)	1839(3)	2729(3)	−1264(1)	65(1)
C(6)	2047(3)	127(3)	1526(1)	58(1)	C(16)	2787(3)	1823(3)	−825(1)	65(1)
C(7)	630(2)	2058(2)	747(1)	43(1)	C(17)	2393(2)	1625(3)	−169(1)	54(1)
					Structure **V**				
O(1)	7189	988(8)	3206	105(6)	C(6)	3162(32)	−814(13)	1056(14)	65(4)
N(1)	6341(61)	−5716(10)	3376(17)	105(6)	C(7)	3023(43)	−2560(14)	1212(17)	75(5)
N(2)	104(79)	−6670(18)	0(23)	140(8)	C(8)	3497(69)	−3488(10)	1583(16)	96(8)
C(1)	4067(31)	−1663(10)	1712(11)	57(4)	C(9)	2248(43)	−4298(13)	973(17)	74(5)
C(2)	5930(49)	−1596(11)	2873(13)	79(5)	C(10)	2671(51)	−5193(11)	1289(15)	80(6)
C(3)	7070(57)	−690(13)	3373(16)	91(6)	C(11)	4797(62)	−5515(12)	2472(17)	88(6)
C(4)	6061(47)	143(13)	2691(15)	75(5)	C(12)	1411(96)	−6041(17)	642(21)	139(13)
C(5)	4140(49)	93(13)	1510(15)	80(5)	C(13)	6080(66)	1894(16)	2654(21)	111(8)

[a] Equivalent isotropic *U* defined as one-third of the trace of the orthogonalized U_{ij} tensor.

was used in our measurements (see below), the influence of the solvent should be much smaller. It was shown[17] for a series of earlier studied derivatives of DIVA that a factor of 2.0 was a good adjustment parameter to account for both the solvent (1,4-dioxane) and dispersion (1064 nm) effects in comparison to the calculated static and measured values of β.

Optical NLO Measurements for Compounds III and V: In Solution. The vector part of the second-order molecular polarizability along the direction of the dipole moment was measured using a nonconventional electric field-induced second-harmonic generation (EFISH) experiment.[17,33] The source was a pulsed Nd:YAG laser (Spectra-Physics Quanta-Ray DCR-11 with near Gaussian optics) operating in the Q-switch mode at a wavelength of 1064 nm at a 10-Hz repetition rate. The single-pulse duration was about 10 ns. Since the laser beam was focused on the sample, less than 5 mJ of energy was sufficient; higher energy laser pulses were known to damage the cell windows and the quartz crystals used in experiments. Details of the modified EFISH technique have been described.[17,33] A similar experimental setup has also been described.[34]

Our EFISH technique has some advantages in comparison with the conventional one. In our cell, the static electric field exists only inside the liquid, and hence any contribution of induced second harmonic inside the glass windows was prevented. Therefore no more additional experiments were required to characterize the nonlinearity of the glass windows. In the conventional EFISH work, great care had to be taken to obtain a uniform DC electric field. In the new system, however, the use of conductive thin films as electrodes and the availability of a larger surface area on the windows in the cell allow one to obtain a uniform field. Moreover, the thin glass spacer between the windows (electrodes) allows one the creation of a static electric field as large as 100 kV/cm. The high DC field and the absence of induced second-harmonic generation make

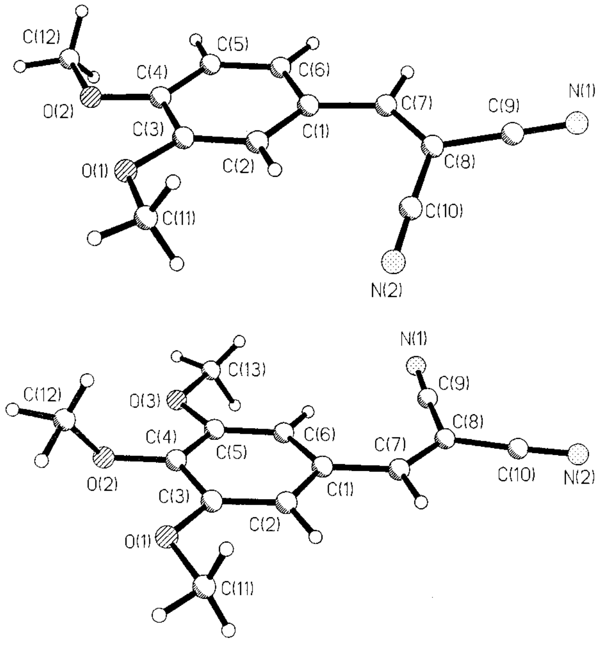

Figure 1. General view of molecular structures of **I** and **II** and atomic numbering schemes.

possible the use of very dilute solutions but with an improved signal-to-noise ratio. In this work we have used concentrations as low as 0.02 M. Uemiya et al.[34] have used concentrations as low as 0.053 M with a similar experimental setup.

Both compounds **III** and **V** were dissolved in 1,4-dioxane. The error associated with the local field correction factors could be minimized by choosing this particular nonpolar solvent. Such a solvent was also required because of the application of high electric field. Furthermore, because of the centrosymmetric structure of 1,4-dioxane, the contribution to the second-harmonic signal by the solvent was zero. The solubility of both compounds **III** and **V** in 1,4-dioxane was poor. Concentration ranges used for these compounds were 0.020−0.040 and 0.040−0.065 M, respectively. Both compounds showed some absorption at the second-harmonic frequency, and therefore appropriate corrections were made to take the absorption into account. In addition, the solute−solute interactions were also taken into account using an infinite dilution method.[35] As a reference material *p*-nitroaniline was used which had been calibrated with a quartz crystal.

The d_{11} value we used for quartz was 0.47 pm/V. In the original paper on the EFISH method published by Levine and Bethea,[36] a similar d_{11} value was accepted to be 0.30 pm/V. There is a number of unresolved inconsistencies in the field of nonlinear optics, and the use of different values for d_{11} of quartz is one of them. The value $d_{11} = 0.47$ pm/V was suggested in the study by Choy and Byer,[37a] and it is based on parametric fluorescence measurements. Many research groups have been using it as the standard since then. However, more recent works performed by Mito et al.[37b,c] and using the SHG technique have reported the d_{11} for quartz to be 0.30 pm/V. The inconsistencies of these standard references are discussed in detail in a very recent publication.[37d] In this work we have used the old value of $d_{11} = 0.47$ pm/V to be consistent with our preliminary measurements and for comparison with the other data. Thus, the β value obtained for MNA and using our EFISH technique (in 1,4-dioxane, ($\lambda = 1064$ nm) was found to be $66.1 \pm 1.1 \times 10^{-51}$ cm^3/V^2, and it agrees well with the value $61.9 \pm 1.9 \times 10^{-51}$ cm^3/V^2 reported by Teng and Garito[38] using the same solvent and wavelength, but the conventional EFISH measurements.

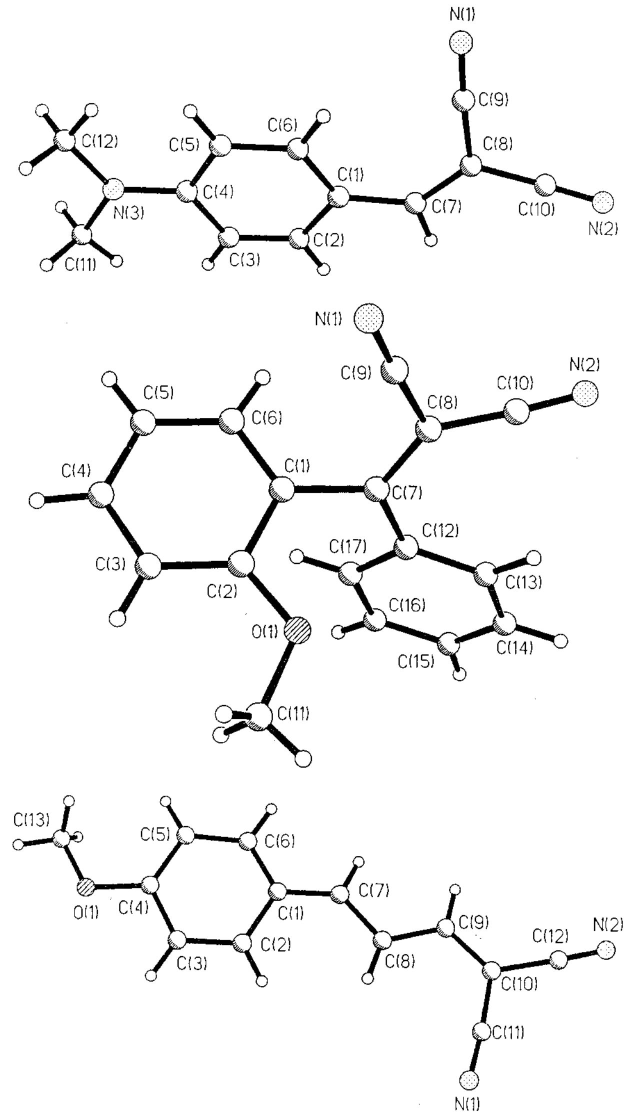

Figure 2. General view of molecular structures **III**−**V** and atomic numbering schemes.

The values of the second-order molecular polarizabilities measured for compounds **III** and **V** were found to be $145.5 \pm 9.1 \times 10^{-51}$ and $90.9 \pm 3.0 \times 10^{-51}$ cm^3/V^2, respectively. Calculated and measured (if any) values of β for all compounds of the series studied are summarized in Tables 5 and 6. The second-order nonlinearities for some of the materials studied were also measured[39] using the conventional EFISH method. However, the fundamental wavelength and the solvents were different from ours, and therefore a mere comparison of results may not make much sense unless the dispersion and solvent effects and other experimental conditions are properly taken into account.

Measurements in the Powder State. Second-harmonic generation efficiency of powder samples of compounds **III** and **V** was measured and compared qualitatively using an experimental setup based on the Kurtz technique at wavelengths of 1064 and 1907 nm. The 1907-nm light was generated using a Raman shifter (metal cylindrical cell, 2.5-cm diameter and 30-cm length, filled with highly pure hydrogen gas at a pressure of about 7.3 MPa). Assuming that the temporal output of the 1064-nm beam exhibited fast mode beating associated with the multilongitudinal mode output, a resonator-type configuration was chosen to alleviate problems with output beam profile, divergence, and pointing stability, which may be caused by the high power of the fundamental beam. The Raman shifter consisted of a converging lens with a focal length of 24 cm used as the input window so the incoming collimated laser beam could be focused at the center of the cell. The design was somewhat different from that of conventional Raman shifters. Its configuration was somewhat similar to that of optical resonator, and 1907-nm light was collected through the input window as backscattered radiation. A rotating glass wedge operated by a DC motor was placed about 10 cm from the input window of the cell. The refraction of the laser beam by the rotating wedge allowed slight displacements of the focal point in the gas. The Raman antistokes at 1907 nm and any backscattering at 1064 nm due to Brillouin scattering were separated by using a dicroic mirror placed at the incidence angle of 45°. Any residual 1064-nm radiation which transmitted through the mirror was blocked by using a 1.0-mm thick Schott BG-18 broad-band filter which showed an extremely good attenuation at 1064 nm and good transmission at 1907 nm. A Corning 7-56 infrared transmitting visible absorbing filter which has a transmission window between 750 and 2700 nm was used to block any visible light.

Powder samples with almost the same particle size were mounted on glass slides and mounted at the focal point of a parabolic mirror, and the scattered second-harmonic light was collected and converged toward a photomultiplier tube. A reference channel was also used to monitor any intensity fluctuations of the laser. SHG signals were detected after filtering them to remove remaining fundamental light and any spurious signals by using broad-band and interference filters. Neutral density filters were also used to attenuate the signal in order to avoid any detector saturation. The 532- and 953-nm SH signals were measured with R268UH and R1527 (Hamamatsu) photomultiplier tubes, respectively.

The second-harmonic light with the wavelength of 532 nm generated by compound **V** was very strong (about 12 times that of urea) and was able to be detected easily with the naked eye. We did not find in the literature any indications about SHG activity for this compound in the solid state, and therefore it may be of interest for further studies. On the contrary, the corresponding SHG signal by the powder of **III** was weak (0.1 times that of urea) and barely visible at high power. Taking into account the relatively large molecular value of β for this compound and close to the "optimal" molecular packing array in its crystal (see below), this result may be explained probably by the strong absorption in **III** near the second-harmonic light. This was proven by the similar SHG measurements at another wavelength of 1907 nm. In this case the second-harmonic light at 953 nm was found to be rather strong for both compounds (10 and 13 times that of urea for **III** and **V**, respectively). Therefore, the low SHG efficiency at 1064 nm in compound **III** seems to be attributed to its strong absorption at 532 nm. Indeed, the measured λ(max) value for this compound in solution was found to be 431 nm which is relatively close to the second-harmonic signal taking into account that a red shift of the shortest cutoff wavelength by as much as 100 nm may occur in the condensed phase.[11] We should note, however, that our results on the SHG test for these two compounds are only qualitative because no analysis of particles size on the SHG efficiency has been done.

Results and Discussion

Molecular Structures and Geometry. Molecular geometry parameters of the compounds studied are not unexceptional (see Figures 1 and 2 and Table 3). Some interesting features of the crystal structures studied should be noted, however.

The molecule of the 3,4-dimethoxy derivative of dicyanovinylbenzene (structure **I**) is almost planar with the interplanar angle between the atoms of the cyano group (coplanar within 0.011 Å) and substituted phenyl ring (atoms of this fragment are coplanar within 0.014 Å) equal to 14.1°. On the contrary, in the structure of **II** two of the three OMe groups in the third and fifth positions of the ring are coplanar with the ring, while the methyl group of the para-substituent is moved out of the ring plane with the torsion angle C(3)−C(4)−O(2)−C(12) equal to 65.8°. Corresponding interplanar angle between the planar cyano-group (0.022 Å) and phenyl ring with its coplanar substituents (0.032 Å) is equal to 5.4°. In the almost planar structure of **III** the angle between these two fragments is equal to 7.7°.

The presence of the phenyl ring at the C(7) atom of the dicyanovinyl group (structure **IV**) prevents molecular planarity. The angles between the planes of the cyano and phenyl and methoxyphenyl groups are equal to 30.3° and 69.3°, and the angle between the two rings is 78.4°. This nonplanarity causes changes in the molecular geometry (see Table 3) and decreases the calculated values of β(see below).

The molecule of **V** in the crystal is also planar within 0.025 Å, but relatively low accuracy of diffraction data due to the crystal twinning excludes more detailed discussion of the molecular geometry of this compound.

Among other features of the molecular geometry of the compounds studied, we will note an increase of the bond angle C(1)−C(7)−C(8) at the vinyl C(7) atom up to 130−135° in comparison with the normal value of 120° (with one exception for the structure of **IV**) that may be related to the intramolecular C(phenyl)−H···N≡C interaction (or interaction between the hydrogen atoms at the C(2) and C(8) atoms in the structure of **V**). The similar feature of the molecular geometry for a given series of compounds was also noted.[17] In the structure of **IV** bond angles at the C(7) atom are closer to the "normal" value of 120° because of nonplanarity of the rings and absence of corresponding intramolecular contacts mentioned above. On the other hand, the C(7)−C(ring) distances equal to 1.484(2) Å for the C(1)−C(7) bond and 1.478(2) Å for the C(7)−C(12) bond are significantly longer (by 0.04−0.06 Å) than the corresponding C(7)−C(ring) bond lengths in other structures of this series.

We should note also the distinguished bond length distributions in the aromatic rings in some of the structures studied. Thus, in the molecule of **I** a clear quinoid character of the benzene ring is evident in the C−C bond lengths: the C(2)−C(3) and C(5)−C(6) bonds are shortened to 1.359(3) and 1.380(3) Å, while the other C−C ring bond lengths are in the interval 1.392(2)−1.419(2) Å. At the same time, the O(2)−C(4) distance of 1.347(3) Å is shorter than the O(1)−C(3) that is equal to 1.373(2) Å. So, the charge transfer in this molecule probably takes place from the para O(2) atom to the dicyanovinyl group. This feature of the molecular geometry agrees well with the calculated values of β (see Table 5 and discussion below) and the fact[17] that the presence of the OMe group in the ortho- or meta-position to dicyanovinyl fragment does not influence significantly the molecular hyperpolarizability.

Very similar quinoid bond length distributions in the aromatic ring are observed also in the structure of **II**. However, the O(2)−C(4) bond is not shortened in this structure, which may be related to the nonoptimal orientation of the corresponding OMe substituent for conjugation (the Me group of this sub-

TABLE 3: Bond Lengths (Å) and Bond Angles (deg) in the Structures Studied

Structure **I**							
O(1)−C(3)	1.373(2)	O(1)−C(11)	1.429(2)	C(1)−C(7)	1.437(3)	C(2)−C(3)	1.359(3)
O(2)−C(4)	1.347(3)	O(2)−C(12)	1.439(3)	C(3)−C(4)	1.419(2)	C(4)−C(5)	1.392(2)
N(1)−C(9)	1.141(3)	N(2)−C(10)	1.144(2)	C(5)−C(6)	1.380(3)	C(7)−C(8)	1.350(3)
C(1)−C(2)	1.419(2)	C(1)−C(6)	1.400(3)	C(8)−C(9)	1.441(3)	C(8)−C(10)	1.439(2)
C(3)−O(1)−C(11)	116.3(2)	C(4)−OI(2)−C(12)	117.7(2)	O(2)−C(4)−C(5)	125.5(2)	C(3)−C(4)−C(5)	118.8(2)
C(2)−C(1)−C(6)	117.8(2)	C(2)−C(1)−C(7)	124.3(2)	C(4)−C(5)−C(6)	120.3(2)	C(1)−C(6)−C(5)	121.4(2)
C(6)−C(1)−C(7)	117.8(2)	C(7)−C(2)−C(3)	121.0(2)	C(1)−C(7)−C(8)	130.6(2)	C(7)−C(8)−C(9)	120.2(2)
O(1)−C(3)−C(2)	125.1(2)	O(1)−C(3)−C(4)	114.2(2)	C(7)−C(8)−C(10)	125.6(2)	C(9)−C(8)−C(10)	114.2(2)
C(2)−C(3)−C(4)	120.7(2)	O(2)−C(4)−C(3)	115.7(1)	N(1)−C(9)−C(8)	179.6(2)	N(2)−C(10)−C(8)	178.7(2)
Structure **II**							
O(1)−C(3)	1.352(5)	O(1)−C(11)	1.456(6)	C(1)−C(7)	1.442(6)	C(2)−C(3)	1.373(6)
O92)−C(4)	1.367(5)	O(2)−C(12)	1.437(7)	C(3)−C(4)	1.425(6)	C(4)−C(5)	1.386(6)
O(3)−C(5)	1.379(5)	O(3)−C(13)	1.438(6)	C(5)−C(6)	1.369(6)	C(7)−C(8)	1.361(6)
N(1)−C(9)	1.153(6)	N(2)−C(10)	1.147(6)	C(8)−C(10)	1.433(7)	C(8)−C(9)	1.439(7)
C(1)−C(6)	1.400(6)	C(1)−C(2)	1.405(6)				
C(3)−O(1)−C(11)	116.5(4)	C(4)−O(2)−C(12)	116.1(4)	C(5)−C(4)−C(3)	119.4(4)	C(6)−C(5)−O(3)	123.9(4)
C(5)−O(3)−C(13)	117.4(4)	C(6)−C(1)−C(2)	118.9(4)	C(6)−C(5)−C(4)	121.8(4)	O(3)−C(5)−C(4)	114.4(4)
C(6)−C(1)−C(7)	124.6(4)	C(2)−C(1)−C(7)	116.5(4)	C(5)−C(6)−C(1)	119.6(4)	C(8)−C(7)−C(1)	131.5(4)
C(3)−C(2)−C(1)	121.9(4)	O(12)−C(3)−C(2)	126.2(4)	C(7)−C(8)−C(10)	119.5(4)	C(7)−C(8)−C(9)	126.1(4)
O(1)−C(3)−C(4)	115.5(4)	C(2)−C(3)−C(4)	118.3(4)	C(10)−C(8)−C(9)	114.4(4)	N(1)−C(9)−C(8)	177.2(5)
O(2)−C(4)−C(5)	119.7(4)	O(2)−C(4)−C(3)	120.8(4)	N(2)−C(10)−C(8)	177.4(5)		
Structure **III**							
N(1)−C(9)	1.143(18)	N(2)−C(10)	1.158(13)	C(2)−C(3)	1.357(14)	C(3)−C(4)	1.427(16)
N(3)−C(4)	1.383(13)	N(3)−C(11)	1.467(20)	C(4)−C(5)	1.409(20)	C(5)−C(6)	1.398(14)
N(3)−C(12)	1.439(15)	C(1)−C(2)	1.410(19)	C(7)−C(8)	1.356(19)	C(8)−C(9)	1.440(19)
C(1)−C(6)	1.406(16)	C(1)−C(7)	1.421(14)	C(8)−C(10)	1.445(14)		
C(4)−N(3)−C(11)	121.2(10)	C(4)−N(3)−C(12)	122.4(12)	C(3)−C(4)−C(5)	119.4(9)	C(4)−C(5)−C(6)	119.9(11)
C(11)−N(3)−C(12)	116.4(9)	C(2)−C(1)−C(6)	116.3(9)	C(1)−C(6)−C(5)	121.5(13)	C(1)−C(7)−C(8)	133.0(11)
C(2)−C(1)−C(7)	119.4(10)	C(6)−C(1)−C(7)	124.4(12)	C(7)−C(8)−C(9)	124.8(9)	C(7)−C(8)−C(10)	120.0(11)
C(1)−C(2)−C(3)	124.7(11)	C(2)−C(3)−C(4)	118.2(12)	C(9)−C(8)−C(10)	115.1(12)	N(1)−C(9)−C(8)	175.0(14)
N(3)−C(4)−C(3)	120.6(12)	N(3)−C(4)−C(5)	119.9(10)	N(2)−C(10)−C(8)	178.4(13)		
Structure **IV**							
O(1)−C(2)	1.354(2)	O(1)−C(11)	1.421(3)	C(7)−C(12)	1.478(2)	C(8)−C(9)	1.436(2)
N(1)−C(9)	1.132(3)	N(2)−C(10)	1.135(3)	C(8)−C(10)	1.431(2)	C(12)−C(13)	1.392(2)
C(1)−C(2)	1.397(2)	C(1)−C(6)	1.381(3)	C(12)−C(17)	1.391(3)	C(13)−C(14)	1.389(3)
C(1)−C(7)	1.484(2)	C(2)−C(3)	1.392(2)	C(14)−C(15)	1.379(3)	C(15)−C(16)	1.372(3)
C(3)−C(4)	1.372(3)	C(4)−C(5)	1.380(3)	C(16)−C(17)	1.386(3)		
C(5)−C(6)	1.384(3)	C(7)−C(8)	1.359(2)				
C(2)−O91)−C(11)	118.0(2)	C(2)−C(1)−C(6)	119.4(2)	C(7)−C(8)−C(9)	120.4(2)	C(7)−C(8)−C(10)	126.0(2)
C(2)−C(1)−C(7)	120.0(2)	C(6)−C(1)−C(7)	120.6(2)	C(9)−C(8)−C(10)	113.6(2)	N(1)−C(9)−C(8)	177.5(2)
O(1)−C(2)−C(1)	115.3(1)	O(1)−C(2)−C(3)	125.2(2)	N(2)−C(10)−C(8)	176.0(2)	C(7)−C(12)−C(13)	122.9(2)
C(1)−C(2)−C(3)	119.4(2)	C(2)−C(3)−C(4)	120.1(2)	C(7)−C(12)−C(17)	118.2(1)	C(13)−C(12)−C(17)	118.9(2)
C(3)−C(4)−C(5)	121.0(2)	C(4)−C(5)−C(6)	119.0(2)	C(12)−C(13)−C(14)	120.4(2)	C(13)−C(14)−C(15)	119.9(2)
C(1)−C(6)−C(5)	121.1(2)	C(1)−C(7)−C(8)	117.5(1)	C(14)−C(15)−C(16)	120.2(2)	C(15)−C(16)−C(17)	120.5(2)
C(1)−C(7)−C(12)	118.2(1)	C(8)−C(7)−C(12)	124.2(1)	C(12)−C(17)−C(16)	120.2(2)		
Structure **V**							
O(1)−C(4)	1.35(2)	O(1)−C(13)	1.43(2)	C(3)−C(4)	1.40(3)	C(4)−C(5)	1.40(2)
N(1)−C(11)	1.12(2)	N(2)−C(12)	1.19(3)	C(5)−C(6)	1.39(2)	C(7)−C(8)	1.35(2)
C(1)−C(2)	1.37(2)	C(1)−C(6)	1.39(2)	C(8)−C(9)	1.36(2)	C(9)−C(10)	1.29(2)
C(1)−C(7)	1.40(2)	C(2)−C(3)	1.42(2)	C(10)−C(12)	1.42(3)	C(10)−C(11)	1.51(3)
C(4)−O(1)−C(13)	121(2)	C(2)−C(1)−C(6)	118.5(13)	C(5)−C(6)−C(1)	122.8(12)	C(8)−C(7)−C(1)	135(2)
C(2)−C(1)−C(7)	120.9(13)	C(6)−C(1)−C(7)	120.6(11)	C(7)−C(8)−C(9)	128(2)	C(10)−C(9)−C(8)	130(2)
C(1)−C(2)−C(3)	121.3(14)	C(4)−C(3)−C(2)	118(2)	C(9)−C(10)−C(12)	130(2)	C(9)−C(10)−C(11)	123(2)
O(1)−C(4)−C(3)	116(2)	O(1)−C(4)−C(5)	122(2)	C(12)−C(10)−C(11)	107(2)	N(1)−C(11)−C(10)	177(2)
C(3)−C(4)−C(5)	122(2)	C(6)−C(5)−C(4)	118(2)	N(2)−C(12)−C(10)	171(3)		

stituent deviates from the ring plane). In the structure of **III** we may note some quinoid character of the ring as well as the shortened C−NMe$_2$ bond length to 1.38(1) Å, but the accuracy of the data is not high enough to make more definite conclusions.

Molecular Dimer Calculations and Crystal Packing Analysis. Calculated energies of the optimized molecular dimers for planar molecules **I**−**III** and **V** are listed in Table 4.

The energy differences between the dimers with starting parallel orientation and having starting C_i and C_2 symmetries are positive and significant for all dimers studied, so their parallel orientation is not preferable in a free state. This is quite understandable, because all molecules under investigation have rather big dipole moments (Table 5), and therefore their parallel orientation may be stabilized only by the strong influence of the crystalline environment. On the contrary, the energy differences between the dimers having C_i and C_2 starting symmetries are not very large. Nevertheless it should be pointed out that for molecules **I** and **II** the dimers with C_i symmetry are more preferable and the energy difference for these dimers in comparison with those with C_2 symmetry is of the same magnitude as for the earlier studied isomer of **I**−2,4-dimethoxy-

TABLE 4: Relative Top List Energies (kcal/mol) of Molecular Dimers with the Initial C_i, C_2, and Parallel Molecular Orientation Symmetries Found as a Result of Stochastic Search

	relative molecular orientation		
molecule	C_i	C_2	parallel
I	0.00	0.23	1.03
	0.09	0.36	1.13
	0.18	0.65	1.20
	0.26	0.96	1.28
	0.33	1.06	1.36
II	0.00	0.25	3.49
	0.09	0.33	3.51
	0.17	0.44	3.73
	0.30	0.54	3.87
	0.41	0.63	3.95
III	0.00	0.06	4.29
	0.13	0.17	4.40
	0.20	0.26	4.51
	0.29	0.38	4.73
	0.60	0.48	4.82
V	0.03	0.00	2.81
	0.12	0.17	2.90
	0.21	0.24	2.92
	0.34	0.36	3.00
	0.44	1.08	3.09

dicyanovinylbenzene.[17] So, according to our calculations, molecules **I** and **II** should be crystallized probably in the centrosymmetric space group that was found experimentally.

For molecules **III** and **V** the energy difference between the C_i and C_2 dimers was found to be negligible; therefore one might not exclude for these compounds a formation of either acentric or centrosymmetric crystals. Our X-ray data showed that these molecules form acentric monoclinic crystal structures with the space groups $P2_1$ and Pc, respectively.

Summarizing results of the dimer calculations, we should note that even such a simple test provides some reasons to exclude from the prospective crystalline SHG materials compounds **I** and **II**, while compounds **III** and **V** may represent some interest in this respect. On the other hand, it is quite clear that the molecular packing pattern will be predetermined not only by the isolated dimer structures but mainly by the sum of all intermolecular interactions in a crystal. Therefore results of our calculations should be considered only as feasible ones. It should be mentioned, however, that for some other dimers consisting of larger and elongated molecules (for example, for 3-amino-3-morpholinyl-2-(*o*-nitrophenylazo)propenonitrile) the difference between the C_i and C_2 dimers is more significant (~6 kcal/mol in preference for C_i dimer), and C_i computed dimers were found to be very close to those found in the crystal.[40] Similar calculations for two known NLO compounds with bulky substituents, namely, 2-(cyclooctylamino)-5-nitropiridine (COANP) and 2-(adamantylamino)-5-nitropiridine (AANP), showed the large preference of the C_2 dimers in comparison with the C_i ones, and these compounds were found to form acentric crystals.[41]

Molecular dimers and crystal packing diagrams for the structures of **I** and **II** are presented in Figures 3 and 4. In particular, Figure 3, top, shows a dimer fragment that may be distinguished in the crystal structure of **I**. The mutual molecular orientation in this dimer and the distance between the planar molecules (3.51 Å) are rather close to the calculated ones. Figure 3, bottom (projection down the *c*-crystal axis), shows that it is possible to separate in this structure centrosymmetric ribbons formed by the relatively weak intermolecular C−H···N≡C "in-plane" interactions (C−H groups belong to the vinyl group and aromatic ring). Geometrical parameters of these interactions [distances (Å) N(1)···H(7′) 2.55, N(1)···C(7′) 3.48, N(2)···H(5′) 2.59, and N(2)···C(5′) 3.36; primed atoms H(7′), C(7′) and H(5′), C(5′) are related with the basis ones in Table 2 by the symmetry transformations (−1−*x*, 1−*y*, 1−*z*) and (*x*, 1 + *y*, *z*)] correspond to the weak hydrogen bonds C−H···N that may stabilize the centrosymmetric crystal structure. Similar hydrogen bonds were found to be important also for some other meta- and para-substituted derivatives of dicyanovinylbenzene,[17] probably indicating that the interactions mentioned prevent crystal structure acentricity.

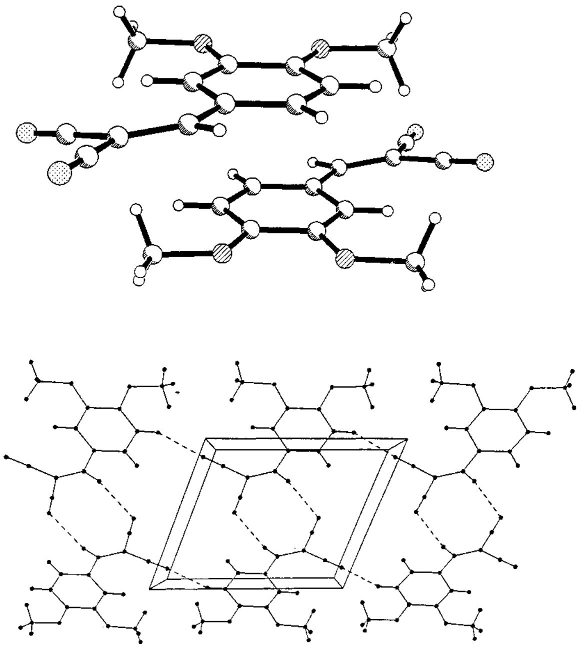

Figure 3. (top) Fragment of the crystal structure of **I** showing the formation of the centrosymmetric "stacking-type" dimer. (bottom) Crystal packing diagram of **I** down the *c*-axis.

In the crystal structure of **II** corresponding C−H···N interactions are present also and have similar geometrical parameters. Because of the presence of three OMe substituents in the ring, these hydrogen bonds join molecules of **II** only in the planar centrosymmetric dimers but not in layers or ribbons. Each N(2′) atom participates as the H atom acceptor in two weak hydrogen bonds, C(2)−H(2)···N(2′) and C(7)−H(7)···N(2′), with the parameters H(2,7)···N(2′) 2.63 and 2.65 Å, angles at the H(2,7) atoms 155° and 151°, and C(2,7)···N(2′) distances 3.559 and 3.616 Å [atom N(2′) is related with the basis one by the symmetry transformation (−*x*, 1−*y*, −*z*)]. It is possible also to distinguish in this structure the "stacking-like" parallel centrosymmetric dimers with the overlap of dicyanovinyl fragments, but not the rings as was obtained in the calculation of free dimers. Crystal structure projection of **II** down the *b*-axis is presented in Figure 4.

Structures **III** and **V** belong to the noncentrosymmetric space groups $P2_1$ and Pc, and the crystal packing analysis is important for understanding their NLO properties in the solid state. Figure 5 shows partial projections of crystal structures of **III** and **V** down the crystal *a*-axes.

In the crystal structure of **III** the orientation of the long molecular axis with respect to the polar crystal axis (*Y*) is close to the expected value for exhibiting high NLO responses. The angle between the polar crystal axis and the N(3)−C(8) line, which might be a possible charge-transfer direction in the molecule, is equal to 59.3°, which is close to the "optimal" value

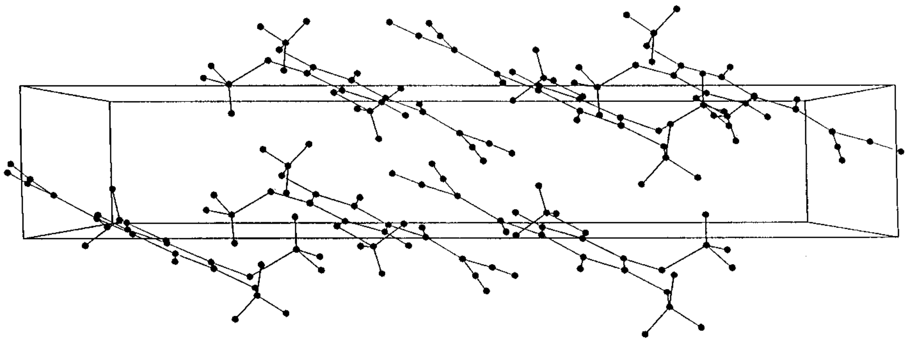

Figure 4. Crystal packing diagram of structure **II** down the *b*-axis.

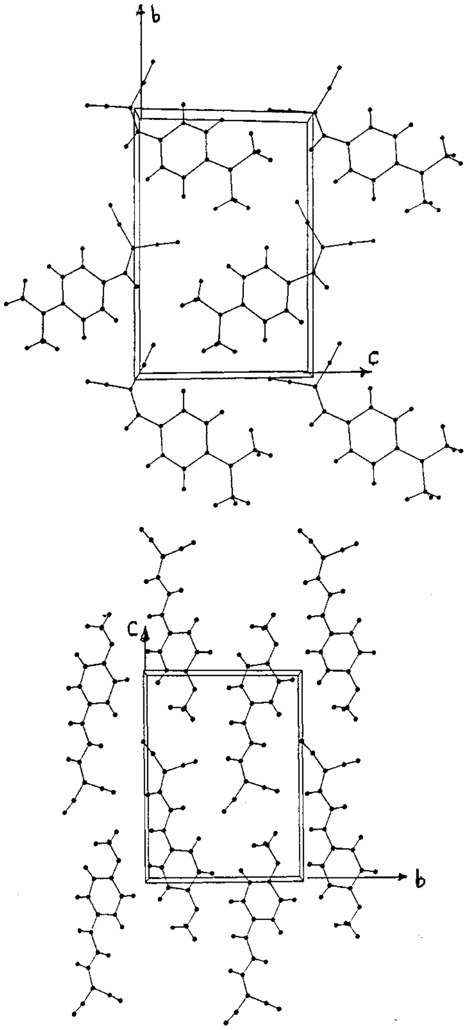

Figure 5. Crystal packing diagrams for structures **III** (top) and **V** (bottom) down the *a*k-crystal axes.

of 54.7° for the space group $P2_1$.[9] So, we may suggest that this compound may be effective as a SHG material in the solid state as was noted shortly.[21] The absence of a strong SGH signal at 532 nm for the powder sample of **III** (see above) is related with the strong absorption that was proven by an additional SHG test at 1907 nm.

In the crystal of **V** (space group *Pc*, $Z = 2$, point group symmetry *m*) the orientation of the mean molecular plane is almost perpendicular to the unique *b*-crystal axis (87.8°). Corresponding angles between this plane and the *a*- and *c*-axes are equal to 148.8° and 54.8°, respectively. Orientation of the molecular dipole moment ($\mu = 6.45$ D in accord with our ab initio STO-3G calculation) is close to the C(5)−N(1) line and does not coincide with the longest molecular axis. The angles between the dipole moment direction and crystallographic *a*,*b*,*c*-axes are 84.4°, 166.2°, and 77.8°, respectively. In the polar (*ac*) crystal plane the angle between the two molecules in the unit cell is 152.3°, and this compound was found be active in the SHG process, in accord with the crystal packing array.[9] It was found earlier[39] that λ(max) band for compound **V** has a hypsochromic shift to the value of 392 nm; therefore this compound may be a prospective material for future applications.

TABLE 5: Calculated and Experimental Second-Order Polarizabilities (β, 10^{-51} cm^3/V^2) and Dipole Moments (μ, D) for the Studied Dicyanovinyl Aromatic Derivatives

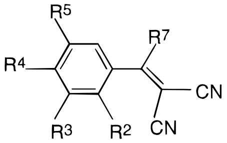

molecule	R^2	R^3	R^4	R^5	R^7	μ	β	exptl β
VI	OMe	H	H	H	H	6.81	12.35	18.71[a]
VII	H	OMe	H	H	H	5.70	19.41	
VIII	H	H	OMe	H	H	4.96	41.98	56.49[a] 36.26[b]
IX	OMe	H	OMe	H	H	6.56	35.68	76.27[a]
I	H	OMe	OMe	H	H	4.87	51.05	78.50[a]
II	H	OMe	OMe	OMe	H	3.98	37.95	
IV	OMe	H	H	H	Ph	5.99	7.59	
X	H	H	OMe	H	Ph	5.83	18.53	
XI	NMe_2	H	H	H	H	5.16	8.49	
III	H	H	NMe_2	H	H	7.21	88.57	145.5 118.7[b]

[a] Reference 17. [b] Reference 37 (measured in $CHCl_3$).

Analysis of Nonlinear Polarizabilities. These calculations were performed in order to reveal relations between the nature of the ring substituents, length of the conjugation chain, and nonlinear optical characteristics of the compounds under investigation. Besides compounds **I**−**V**, the dipole moments (μ, D) and the static second-order polarizabilities (β, 10^{-51} cm^3/V^2) for two groups of the parent compounds were calculated also including substituted derivatives with the dicyanovinyl ($-CH{=}C(CN)_2$) and 1,1-dicyano-1,3-butadiene ($-CH{=}CH-CH-C{=}C(CN)_2$) fragments. Tables 5 and 6 contain calculated values of μ and β together with available experimental data.

Comparison of the mono-, di-, and trisubstituted methoxy-dicyanovinylbenzenes shows that introduction of the two methoxy substituents in 3,4-positions of the aromatic ring (molecule **I**) results in the best result for the molecular hyperpolarizability in this series. Introduction of the third methoxy group (molecule **II**) decreases the hyperpolarizability. The latter may be explained by the molecular nonplanarity. Namely, *p*-methoxy substituent in this molecule (the most important position for exhibiting a high molecular NLO

TABLE 6: Calculated and Experimental Second-Order Susceptibilities (β, 10^{-51} cm^3/V^2) and Dipole Moments (μ, D) for Dicyanovinyl-Substituted Aryl Polyene Molecules

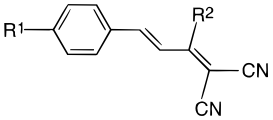

molecule	R^1	R^2	μ	β	exptl β
V	OMe	H	6.46	103.47	90.7 118.7[a]
XII	NMe_2	H	7.18	136.48	304.4[a]
XIII	NEt_2	H	8.46	198.67	
XIV	OMe	CN	6.02	106.92	
XV	NMe_2	CN	8.44	256.75	
XVI	NEt_2	CN	8.52	275.37	

[a] Reference 37.

response) is out of the ring plane, with the corresponding torsion angle C(3)−C(4)−O(2)−C(12) is equal to 65.8° according to the X-ray data and 81.2° as a result of the MM calculation. So, the conjugation and charge-transfer conditions in this case are worse than for molecules **I** and **VIII** having planar OMe groups in the para-position of the ring. Experimental (X-ray) bond length distributions in structures **I** and **II** support this speculation.

It should be mentioned that the hyperpolarizability value calculated earlier for the molecule **I**[17] was slightly different ($44.633 \pm 0.025 \times 10^{-51}$ cm^3/V^2) from that calculated in the present paper ($51.050 \pm 0.040 \times 10^{-51}$ cm^3/V^{-2}). The difference is due to the different conformation of this molecule in calculation that was previously made[17] (both OMe groups pointed in the same direction, while in the present calculation they are pointing in opposite directions, Figure 1, which is in accord with our X-ray data).

The same argument (the loss of conjugation because of molecular nonplanarity) might be pointed out for a decrease of hyperpolarizability in molecule **IV** having the phenyl substituent at the C(7) atom, if comparing the data with that of the corresponding unsubstituted analogue (molecule **VI**, or DIVA). Among all compounds in Table 5, molecule **IV** has the smallest value of β. As a rule, the phenyl group itself is not a group which influences strongly the molecular hyperpolarizability,[42] but in some cases it can produce some effect if steric factors are not involved.[43] It is interesting to note, therefore, that in molecule **X** having the same phenyl substituent at the C(7) atom, but the *p*-OMe substituent in the ring, the value of β is relatively large.

As was shown earlier[21] and in accord with the stronger donor properties of the dimethylamino group, NMe_2 derivatives should have larger hyperpolarizabilities than corresponding OMe-substituted analogues. Indeed, we could demonstrate it for the para-substituted derivatives **III** and **VIII** where corresponding β values differ more than twice in preference of dimethylamino derivative **III**. On the contrary, ortho-substitution (molecules **VI** and **XI**) results in the opposite situation that may be related with the nonplanarity of molecule **XI**. According to the MM calculation, torsion angle C(Ph)−C(Ph)−N−C(Me) characterizing the rotation of the NMe_2 group is equal to 63.2°, which excludes its conjugation with the aromatic ring.

Table 6 contains corresponding data on dipole moments and β values for similar series of aromatic compounds having longer conjugation chains.

It was pointed out in the literature[5,6,39] that an elongation of the conjugation chain in the "push−pull" molecules leads to an increase of the molecular hyperpolarizability. According to the MM calculations all molecules listed in Table 6 are nearly planar. Their hyperpolarizabilities are in accord with a donor−acceptor group capacity and the length of the conjugation chain, and they are much larger than those for the first series of the compounds studied. It should be noted that in this series the molecular hyperpolarizability grows significantly when the OMe group is substituted with a NMe_2 or NEt_2 group. Further studies of this series might be interesting in the search for new NLO materials.

Acknowledgment. This work was supported in part by NASA-IRA Grant NAG5-5121 and by AFOSR Grant F49620-97-1-0256. Thanks are given to Tiffany Myers for part of the synthetic work.

Supporting Information Available: Tables of structure determination summaries (crystal data, data collection conditions, structure solution, and refinement results), tables of non-hydrogen atom coordinates and their equivalent displacement parameters, tables of bond lengths and bond angles, tables of hydrogen atom coordinates and their isotropic displacement parameters, and tables of anisotropic displacement parameters for non-hydrogen atoms (41 pages). Ordering information is given on any currant masthead page.

References and Notes

(1) *Nonlinear Optical Properties of Organic Molecules and Crystals*; Chelma, D. S., Zyss, J., Eds.; Academic Press: Orlando, FL, 1987l Vol. 1.

(2) *Materials for Nonlinear Optics: Chemical Perspectives*; Marder, S. R., Sohn, J. E., Stucky, G. D., Eds.; ACS Symposium Series 455; American Chemical Society: Washington, DC, 1991.

(3) *Molecular Nonlinear Optics: Materials, Physics, and Devices*; Zyss, J., Ed.; Academic Press: New York, 1994.

(4) Lipscomb, G. F.; Garito, A. F.; Narang, R. S. *J. Chem. Phys.* **1981**, *75*, 1509.

(5) Kanis, D. R.; Ratner, M. A.; Marks, T. J. *Chem. Rev.* **1994**, *94*, 195−242.

(6) Long, N. J. *Angew. Chem., Int. Ed. Engl.* **1995**, *34*, 21.

(7) Prasad, P. N.; Reinhardt, B. A. *Chem. Mater.* **1990**, *2*, 660.

(8) Albert, I. D. L.; Marks, T. J.; Ratner, M. A. *J. Chem. Phys.* **1996**, *100*, 9714.

(9) (a) Zyss, J.; Oudar, J. L. *Phys. Rev. A* **1982**, *26*, 2028−2048. (b) Oudar, J. L.; Zyss, J. *Phys. Rev. A* **1982**, *26*, 2016−2027.

(10) Mak, T. C. W.; Trotter, J. *Acta Crystallogr.* **1965**, *18*, 68.

(11) Zyss, J. In *Conjugated Polymeric Materials: Opportunities in Electronics, Optoelectronics and Microelectronics;* Bredas, J.-L., Chance, R. R., Eds.; Kluwer: Dortdrecht, 1990.

(12) Holden, J. R.; Du, Z.; Ammon, H. L. *J. Comput. Chem.* **1993**, *14*, 422−437.

(13) Gavezzotti, A. *Acc. Chem. Res.* **1994**, *27*, 309.

(14) Chaka, A. M.; Zaniewski, R.; Youngs, W.; Tessier, C.; Klopman, G. *Acta Crystallogr. B* **1996**, *B52*, 165.

(15) Wolff, J. J. *Angew. Chem., Int. Ed. Engl.* **1996**, *35*, 2195.

(16) (a) Fkyerat, A.; Guelzim, A.; Baert, F.; Paulus, W.; Heger, G.; Zyss, J.; Perigaud, A. *Acta Crystallogr. B* **1995**, *51*, 197−209. (b) Fkyerat, A.; Guelzim, A.; Baert, F.; Zyss, J.; Perigaud, A. *Phys. Rev. B* **1996**, *53*, 16236−16246.

(17) Antipin, M. Yu.; Barr, T. A.; Cardelino, B.; Clark, R. D.; Moore, C. E.; Myers, T.; Penn, B.; Romero, M.; Sangadasa, M.; Timofeeva, T. V. *J. Phys. Chem.* **1997**, *101*, 2770−2781.

(18) Kanis, D. R.; Marks, T. J.; Ratner, M. A. *Int. J. Quant. Chem.* **1992**, *43*, 61.

(19) Wada, T.; Grossman, G. H.; Yamada, S.; Yamada, A.; Garito, A. F.; Sasabe, H. *Mater. Res. Soc. Symp. Proc.* **1990**, *173*, 519−523.

(20) Wada, T.; Yamada, S.; Matsuoka, Y.; Grossman, C. H.; Shidehara, K.; Sasabe, H.; Yamada, A.; Gartio, A. F. In *Nonlinear Optics of Organic and Semiconductors*; Kobayashi, T., Ed.; Springer: New York, 1989; Vol. 36, p 292.

(21) Matsuoka, M.; Takao, M.; Kitao, T.; Fujiwara, T.; Nakatsu, K. *Mol. Cryst. Liq. Cryst.* **1990**, *182A*, 71−79.

(22) Silver, F.; Kerr, K. A.; Fradsen, P. D.; Kelly, S. J.; Holmes, H. L. *Can. J. Chem.* **1967**, *45*, 101.

(23) Compaigne, E.; Mais, D.; Yokley, E. M. *Synth. Commun.* **1974**, *6*, 379.

(24) Saunders, M. *J. Am. Chem. Soc*. **1987**, *109*, 3150.

(25) (a) Itoh, Y.; Oono, K.; Isogai, M.; Kakuta, A. *Mol. Cryst. Liq. Cryst*. **1989**, *170*, 259−272. (b) Itoh, Y.; Oono, K.; Isogai, M.; Kakuta, A. *SPIE* **1988**, *1017*, 127.

(26) Albert, I. D. L.; Marks, T. J.; Ratner, M. A. *Chem. Mater*. **1998**, *10*, 753−762.

(27) Allinger, N. L.; Yuh, Y. H.; Lii, J.-H. *J. Am. Chem. Soc*. **1989**, *111*, 8551.

(28) Lii, J.-H.; Allinger, N. L. *J. Am. Chem. Soc*. **1989**, *111*, 8566.

(29) Cardelino, B. H.; Moore, C. E.; Frazier, D. O. *J. Phys. Chem*. **1997**, *101*, 2207.

(30) Dewar, M. J. S.; Stewart, J. J. P. *Chem. Phys. Lett.* **1984**, *111*, 416.

(31) Kurtz, H. A.; Stewart, J. J. P.; Dieter, K. M. *J. Comput. Chem*. **1990**, *11*, 82.

(32) (a) Cardelino, B. H.; Moore, C. E.; Stickel, R. E. *J. Phys. Chem*. **1991**, *95*, 8645−8652. (b) Allin, S. B.; Leslie, T. M.; Lumpkin, R. D. *Chem. Mater*. **1996**, *8*, 428−432.

(33) Sanghadasa, M.; Barr, T. A.; Clomenil, D.; Tong, Yu.; Bhat, K.; Clark, R. D.; Penn, B. *Proc. SPIE* **1996**, *2853*, 37.

(34) Uemia, T.; Uenishi, N.; Umegaki, S. *J. Appl. Phys*. **1993**, *73*, 12.

(35) Singer, K. D.; Sohn, J. E.; King, L. A.; Gordon, H. M.; Katz, H. E.; Dirk, H. M. *J. Opt. Soc. Am.* **1989**, *B6*, 1339.

(36) Levine, B. F.; Bethea, C. G. *J. Chem. Phys*. **1975**, *63*, 2666.

(37) (a) Choy, M. M.; Byer, R. L. *Phys. Rev. B* **1976**, *14*, 1693. (b) Mito, A.; Higimoto, K.; Takahashi, C. International Symposium on Nonlinear Photonics Materials, Japan, May 1994; pp 85−99. (c) Mito, A.; et al. *Nonlinear Opt*. **1995**, *13*, 3. (d) Shi, R. F.; Garito, A. F. In *Characterization Techniques and Tabulations for Organic Nonlinear Optical Materials*; Kyzuk, M. G., Dirk, C. W., Eds.; Marcel Dekker Inc. Publ.: New York, 1998; pp 1−36.

(38) Teng, C. C.; Garito, A. F. *Phys. Rev. B* **1983**, *28*, 6766.

(39) Cheng, L. T.; Tam, W.; Marder, S. R.; Steigman, A. E.; Rikken, G.; Spangler, C. W. *J. Phys. Chem*. **1991**, *95*, 10643.

(40) Nesterov, V. N.; Timofeeva, T. V.; Duerksen, G.; Clark, R. D. *J. Mol. Struct.* **1998**, *444*, 135.

(41) Antipin, M. Yu.; Nesterov, V. N.; Timofeeva, T. V.; Clark, R. D. Manuscript in preparation.

(42) Zyss, J. *J. Chem. Phys*. **1979**, *70*, 3341.

(43) Whitaker, C. M.; Patterson, E. V.; Kott, K. L.; McMahon, R. J. *J. Am. Chem. Soc*. **1996,** *118*, 9966.